

## 3D Wave-Current Interactions in Wave-Current Channels

Jacco Groeneweg<sup>1</sup> and Jurjen A. Battjes<sup>1</sup>

### Abstract

*Measurements of mean velocity profiles in a wave-current flume have shown some features for which the mechanism is far from trivial. A 2DV model based on the so-called Generalized Lagrangian Mean formulation is developed to study the influence of waves on the mean motion, the mean horizontal velocity in particular. This influence can be split in two parts, viz. a direct effect of the waves via wave-induced driving forces and an indirect effect of waves via secondary circulations. To include both effects an existing 1DV model is extended by introducing lateral variations including side-wall boundary layers. Resulting formulations have been implemented in an existing 2DV non-hydrostatic numerical flow model. Computations for regular waves following and opposing a turbulent current have been carried out and compared with both experimental results and results from an existing numerical model.*

### Introduction

Understanding the mechanism of wave-current interaction is of great importance for a good prediction of vertical profiles of horizontal velocities. The study of these profiles is relevant from both a hydrodynamic point of view (bed friction), and a morphodynamic point of view. Observations in laboratory experiments by e.g. Kemp & Simons (1982; 1983) and Klopman (1994) of the effect non-breaking waves on a steady turbulent current over a rigid rough bed show significant and unexpected changes in the profiles of the mean horizontal velocity (see figure 1).

To the authors' knowledge only Nielsen & You (1996) and Dingemans *et al.* (1996) presented theoretical models to explain the wave-induced changes in the Eulerian-mean horizontal velocity profiles. The model of Nielsen & You (1996) is based on a local force balance. In a steady two-dimensional flow the

---

<sup>1</sup>Delft University of Technology, Department of Civil Engineering and Geosciences, Stevinweg 1, 2628 CN Delft, The Netherlands.

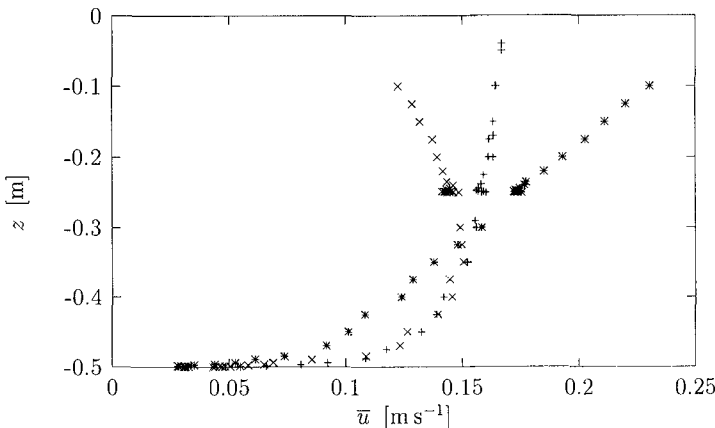


Figure 1: Eulerian-mean velocity profiles for the situation of no waves (+), following waves (x) and opposing waves (\*) of the same size (depth 0.5 m, wave period 1.44 s, wave amplitude 0.06 m). After Klopman (1994).

vertical variation of the total shearing force per unit area of a cross-section was balanced by the horizontal variation of the total normal stress. Assuming linear wave theory, expressions were derived for the mean wave contribution  $\langle \tilde{u}\tilde{w} \rangle$  and for the local radiation stress. Although their model gives a qualitative explanation of the physical mechanisms involved, quantitative agreement with Klopman's results was obtained only after a significant ad hoc enhancement of  $\langle \tilde{u}\tilde{w} \rangle$  by a linearly depth-dependent empirical factor. The empirical adjustment is based on the fact that the interaction with a current induces extra vorticity of the wave motion.

Dingemans *et al.* (1996) developed a 2DV model, the results of which were compared with the wave flume experiments of Klopman (1994). A detailed description of this model is given in the report of Van Kester *et al.* (1996). The effect of waves has been incorporated by adding the so-called Craik-Leibovich (CL) vortex force, consisting of  $\bar{u}^S \times \bar{\omega}$  with  $\bar{u}^S$  the Stokes drift and  $\bar{\omega} = \nabla \times \bar{u}$  the mean vorticity. Among others Leibovich (1983) showed that under certain assumptions the vortex force is the main term in the ensemble-averaged momentum equations in a so-called GLM formulation. Dingemans *et al.* (1996) observed in their simulations that secondary lateral circulations induced by the CL vortex force caused changes in the vertical structure of the mean horizontal flow. However, due to poor estimates of the Stokes drift and the CL vortex force in the boundary layers, quantitative agreement with Klopman's experimental results was not obtained for situations of waves following or opposing

a current.

Groeneweg & Klopman (1998) developed a 1DV model, based on the Generalized Lagrangian Mean (GLM) formulation. This approach, in which the Lagrangian motion is described in a fixed Eulerian framework, has been introduced by Andrews & McIntyre (1978) in order to obtain a clear separation of the mean and fluctuating motion. In the model lateral variations have been neglected. Comparison with Klopman's results shows both qualitative and quantitative agreement.

An intriguing point is that two models of Nielsen & You (1996) and Groeneweg & Klopman (1998) confirm the theory that changes of the mean horizontal velocity profile are purely caused by phenomena in longitudinal direction, whereas Dingemans *et al.* (1996) suppose the secondary lateral circulations to be the reason for changes in the mean horizontal velocity profile in streamwise direction. Their prediction of the existence of lateral circulations is supported by laboratory measurements of Klopman (1997).

The purpose of this work is to develop a 2DV model, which describes the mean flow under the influence of the wave motion, in a Generalized Lagrangian Mean (GLM) formulation in order to provide more insight in the effect of the secondary circulations on the mean horizontal velocity profile. The work is presently in a preliminary state and the results of the developed 2DV model are not yet completely satisfactory. Therefore, the presentation of the model will not be given in detail and frequent reference is made to Groeneweg & Klopman (1998) (to be denoted as GK hereafter). General formulations of the flow equations in a GLM setting as well as a 1DV application of a combined wave-current problem have been given in detail in that paper.

### GLM approach

As already mentioned in the introduction a hybrid Eulerian-Lagrangian approach, the so-called GLM approach, will be adopted to simulate the combined motion of waves and currents in a flume. For the definition of the GLM theory we refer to Andrews & McIntyre (1978), or for an introductory outline to McIntyre (1980) and Dingemans (1997, note 2.10.6). The notation in this paper is exactly the same as applied by GK. Here, only the essential idea of the GLM theory is outlined. A Cartesian coordinate system  $(x, y, z)$  is used, where  $z$  is the vertical direction,  $x$  and  $y$  the horizontal coordinates in longitudinal and lateral direction respectively. Central in the GLM description is the mapping  $\mathbf{x} \rightarrow \mathbf{x} + \boldsymbol{\xi}(\mathbf{x}, t)$ , where  $\boldsymbol{\xi}(\mathbf{x}, t)$  is a field denoting the displacement about the position  $\mathbf{x}$ . By introducing  $\varphi^\xi(\mathbf{x}, t) = \varphi(\mathbf{x} + \boldsymbol{\xi}(\mathbf{x}, t), t)$  for an arbitrary particle-related function  $\varphi$ , Andrews & McIntyre (1978) define a Lagrangian

mean operator  $\overline{(\ )}^L$  by

$$\overline{\varphi(\mathbf{x}, t)}^L = \langle \varphi^\xi(\mathbf{x}, t) \rangle, \quad (1)$$

where in our case  $\langle (\ ) \rangle$  will be a time-average operator. This implies that the average assigned to the fixed point  $\mathbf{x}$  is taken over disturbed positions  $\mathbf{x} + \xi(\mathbf{x}, t)$ . In order that  $\xi$  is a true disturbance, it is required that  $\overline{\xi(\mathbf{x}, t)} = 0$ . The fluctuation  $\varphi^\ell$  is defined in a natural way as  $\varphi^\ell = \varphi^\xi - \overline{\varphi}^L$ , and thus  $\overline{\varphi^\ell} = 0$ . Finally, the difference between the GLM velocity and Eulerian mean velocity is given by the so-called Stokes drift,  $\overline{\mathbf{u}}^S = \overline{\mathbf{u}}^L - \overline{\mathbf{u}}$ . A Stokes correction  $\overline{\varphi}^S$  can be expressed in terms of fluctuating quantities.

In GK the three-dimensional GLM flow equations have been derived in a general way. Therefore, the lateral 2DV model, providing a local solution in a cross-sectional plane, can be obtained just by neglecting variations in longitudinal direction of GLM quantities, except for the hydrostatic part of the GLM pressure which is related to the GLM surface elevation  $\zeta^L$ . The total pressure  $\bar{p}^L$  is decomposed in a hydrostatic and non-hydrostatic part,  $\bar{p}^L = \rho g (\zeta^L - z) + \bar{q}^L$ . The horizontal gradient of the hydrostatic pressure,  $\partial \zeta^L / \partial x$ , is assumed constant over the entire cross-section and chosen such that the discharge of the combined flow equals the discharge  $Q$  of the flow without waves. A cross-section at a distance  $x$  from the wave maker is defined as  $\Omega(x) = \{(y, z) : -L \leq y \leq L, -h \leq z \leq \zeta^L(x, y, t)\}$ . Here we restrict ourselves to vertical side walls and a horizontal bottom profile.

The flow equations in GLM coordinates are of the same form as those in Eulerian formulation. Only the wave-induced driving forces in the momentum equations are different, and a wave-related correction in the continuity equation causes the mean velocity to be no longer divergence free.

The wave-induced driving forces are expressed in terms of fluctuating quantities in GK. The 1DV model presented in that paper provides the vertical profiles of the fluctuating quantities as well. In order to take side wall effects into account we adopt a procedure that was also used by Mei *et al.* (1972), who analyzed mass transport caused by progressive waves for a situation of constant viscosity and no initial current. A cross-section  $\Omega(x)$  of the flume is subdivided into five regions, viz. the inviscid core region and the boundary layers at the bottom, the free surface and the two side walls. This is sketched in figure 2.

Analogous to the analysis of Mei *et al.* (1972) viscous effects are neglected outside the side wall boundary layers. Consequently, the lateral variations of the amplitude functions of the fluctuating quantities can be neglected. The flow equations for the fluctuating motion are then reduced to those derived for the 1DV problem in GK. The solution of the latter problem will be denoted by  $\varphi = \varphi_1$ . Following e.g. Mei *et al.* (1972) one can easily show that the first order first harmonic velocity including the no-slip condition at the side walls

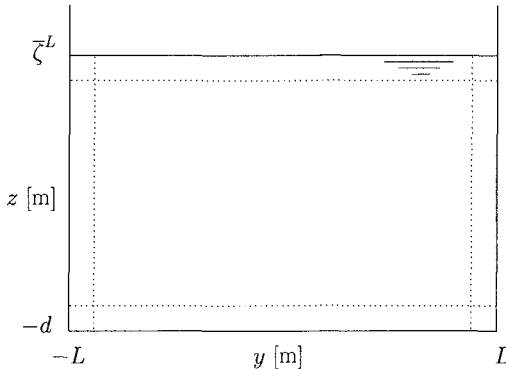


Figure 2: Division of a cross-section  $\Omega(x)$  into five regions.

satisfies Stokes' shear wave solution given by

$$\tilde{u} = [1 - \exp(\beta Y)] \tilde{u}_1 , \quad (2a)$$

$$\tilde{v} = \tilde{v}_1 = 0 , \quad (2b)$$

$$\tilde{w} = [1 - \exp(\beta Y)] \tilde{w}_1 . \quad (2c)$$

with the factor  $\beta = (-i\omega_0/\nu)^{1/2}$  and  $Y$  the distance to the nearest side wall. The influence of the mean current and variations of the eddy viscosity  $\nu$  have been neglected in the side-wall boundary layers. To sum up: the 1DV model is used to determine the vertical distribution of the fluctuating quantities. The 2DV profiles are obtained by multiplying the 1DV profile (subscript 1) by a  $y$ -dependent factor, which only affects the fluctuating motion in the side-wall boundary layers.

The distribution of the wave-induced driving forces in the entire cross-section can now easily be found by substituting the laterally varying oscillating quantities in the general expressions for the driving forces.

#### Implementation of GLM equations in existing numerical model

Although the flow equations are given in a GLM formulation, their form is similar to their Eulerian counterpart. For this reason an Eulerian flow solver can be used to integrate the GLM flow equations. We have chosen for the 2DV non-hydrostatic flow solver developed by Van Kester *et al.* (1996). For the numerics in this model one is referred to *loc. cit.* After the wave-induced driving forces  $\bar{\mathcal{S}}^L$  and the GLM-correction term in the continuity equation have been evaluated, implementation of these terms is straightforward.

The implementation of the boundary conditions at the bottom and side-walls needs special care. In Van Kester *et al.* (1996) partial-slip conditions are imposed at those boundaries, using a logarithmic law-of-the-wall formulation. This type of boundary condition differs from the no-slip condition used in the 1DV model. Therefore, correct expressions had to be determined for these boundary conditions in a GLM setting. For the time being the simplest possible approach has been adopted. The formulation applied by Van Kester *et al.* (1996) is based on a formulation of Grant & Madsen (1979) and takes the presence of the wave motion into account. Given a shear velocity at a certain distance from the wall, the friction velocity and related shear stress are determined. This formulation is given in an Eulerian framework. In order to obtain the GLM shear stress at a closed boundary, the following algorithm has been applied:

1. The GLM velocity at a certain height or distance from the side wall is transformed to its Eulerian equivalent at the same height.
2. The formulation of Grant & Madsen (1979) which has been applied by Van Kester *et al.* (1996), is used to determine the Eulerian shear stress at the boundary.
3. The Eulerian shear stresses are transformed to GLM shear stresses by adding the Stokes correction of the shear stress under consideration.

Finally, for simulating turbulent flow a turbulence model has to be implemented. In a first approach a classical turbulence model has been used. Any of the turbulence models implemented by Van Kester *et al.* (1996) can be used. For this study a  $k - \varepsilon$  model was chosen. In order to take the wave influence into account, boundary conditions for the turbulent kinetic energy and dissipation are related to the shear velocity near the boundary. As mentioned above the shear velocities are determined using a logarithmic law of the wall. For closure of the turbulence model the production term is computed with Eulerian velocities, which are determined by transforming the GLM velocities.

### Model results

Mean velocities have been computed for situations of following and opposing waves. In order to compare the model results with experimental data, the initial conditions of one of Klopman's (1994; 1997) measurements have been applied. In the present model a turbulent current with a constant discharge of  $Q = 0.08 \text{ m}^3 \text{s}^{-1}$  was generated in a 1.0 m wide flume ( $L = 0.50 \text{ m}$ ) with a still-water depth  $h = 0.50 \text{ m}$ . A monochromatic wave field following or opposing the current with a wave period  $T = 1.44 \text{ s}$  (relative to the flume) and wave

amplitude  $a = 0.060\text{ m}$  is superposed on the current. All presented results refer to the situation at  $t = 1600\text{ s}$  and have been obtained on an equidistant grid with horizontal and vertical resolution  $\Delta x = 0.01\text{ m}$ , resp.  $\Delta y = 0.0125\text{ m}$  and a time step  $\Delta t = 0.02\text{ s}$ .

In the present 2DV model the wave-induced driving forces depend via the orbital quantities on the factor  $\beta = (-i\omega/\nu)^{1/2}$ . In our analysis the quantity  $\nu$  was assumed independent of the lateral direction. We have taken  $\nu = 10^{-4}\text{ m}^2\text{ s}^{-1}$  in all experiments, representing a turbulent oscillatory motion. This choice for  $\nu$  leads to a factor  $\beta$  for which  $\text{Re}(\beta) = -(\omega/2\nu)^{1/2} \approx -148\text{ m}^{-1}$ .

Since velocity measurements have been carried out at fixed locations and are thus Eulerian, the GLM velocities  $\bar{\mathbf{u}}^L$  have to be transformed to Eulerian velocities. In this section these are denoted as  $\mathbf{U}$ . As already mentioned  $\mathbf{U} = \bar{\mathbf{u}}^L - \bar{\mathbf{u}}^S$ .

In figure 3 and 4 the results for the mean velocity distribution in a cross-section at  $x = 22.5\text{ m}$  from the wave maker and the mean horizontal velocity profile in streamwise direction in the center of the flume are shown for the situation of waves propagating in the current direction. The agreement with measurements of Klopman (1997) is only qualitative. The direction of the computed secondary circulation is correct, but the velocity magnitude is a factor 2, and at the side walls even a factor 3 larger than measured. Near the side wall the maximum velocity magnitude is  $2.0\text{ cm s}^{-1}$  and in the center  $1.6\text{ cm s}^{-1}$ . The computed secondary circulations are comparable to those obtained by Dingemans *et al.* (1996). The mean horizontal velocity in the center of the flume is fairly well predicted by the 2DV model. Compared with the measurements of Klopman (1994) and the 1DV results of GK there is a slight overprediction in the lower region of the flume and an underprediction in the higher region.

In figure 5 and 6 the results have been plotted for the situation that waves are propagating in the opposite direction. Once again, the maximum velocity magnitude near the side wall is  $2.5\text{ cm s}^{-1}$  and in the center of the flume  $1.8\text{ cm s}^{-1}$ , which is even an overprediction of Klopman's (1997) experimental data with a factor 4 to 5. The prediction of the mean horizontal velocity profile in streamwise direction is even worse. Whereas for the situation of waves following the current at least the trend was predicted correctly, this is not true in the opposite case. In the upper 40% of the flume the velocity gradient seems to vanish whereas the experiments of Klopman (1994) and the 1DV computations of GK show an increasing velocity gradient.

The side walls should have less effect on the mean velocity profile in the center of the flume when a wider flume is considered. The secondary lateral circulations should then decrease in magnitude. Moreover, the 2DV solution should converge to the 1DV solution as  $L \rightarrow \infty$ . However, we remark that

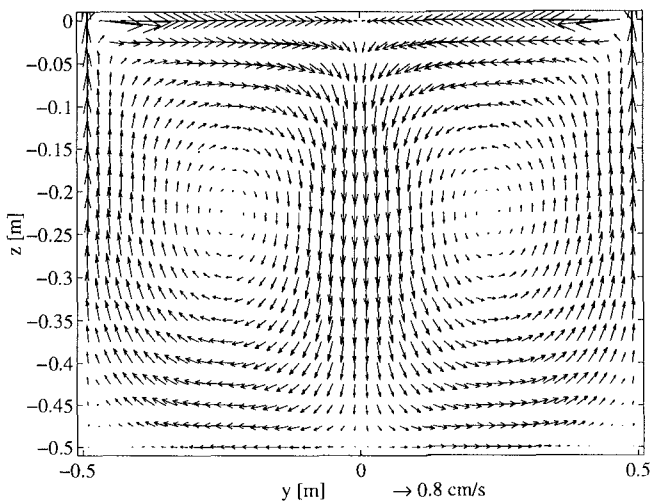


Figure 3: Mean velocity distribution in cross-section for waves following the current. Note difference between horizontal and vertical scale.

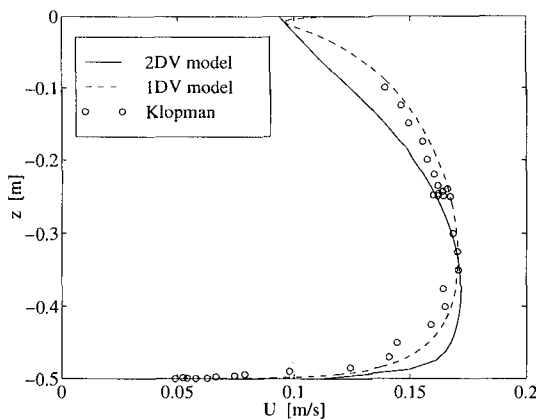


Figure 4: Mean streamwise horizontal velocity profile in center of the flume for waves following the current.

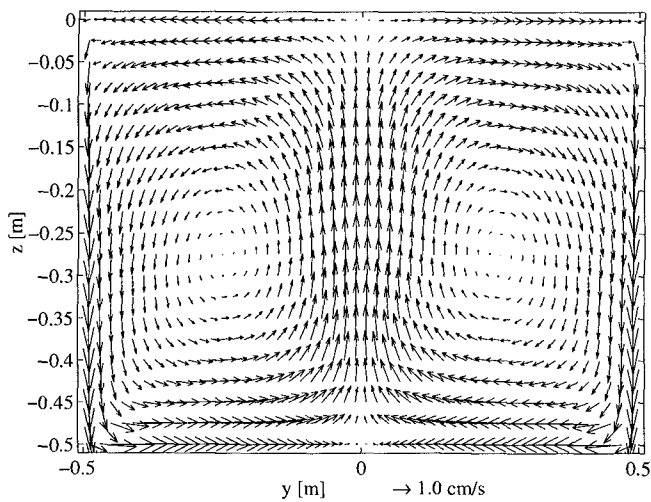


Figure 5: Mean velocity distribution in cross-section for waves opposing the current.

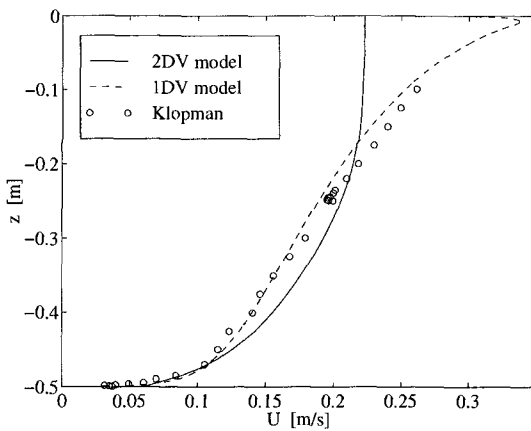


Figure 6: Mean streamwise horizontal velocity profile in center of the flume for waves opposing the current.

some principal differences in the formulation of both models, such as the turbulence model and boundary layer treatment, will induce some differences in the results.

To study the effect mentioned above, the same situation with a following current is considered as before, but now in a 5 m wide flume. The discharge is increased proportionally,  $Q = 0.40 \text{ m}^3 \text{s}^{-1}$ . In figure 7 the velocity distribution is shown only in the region 50 cm from the left side wall. The velocity magnitude is obviously smaller, at most  $0.8 \text{ mm s}^{-1}$ . A circulation cell can still be observed. Our main interest concerns the mean horizontal velocity profile in the center of the flume as given in figure 8. Comparing this with the distribution obtained in a 1 m wide flume only shows a slight difference.

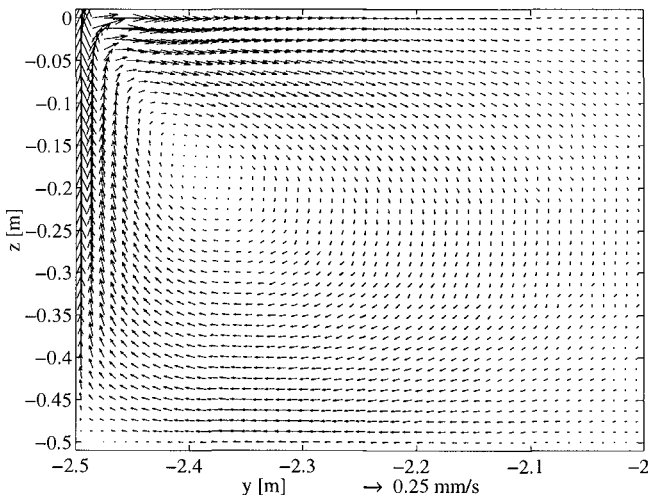


Figure 7: Mean velocity distribution in a part of the cross-section for waves following the current in a 5 m wide flume.

### Discussion

Two important philosophies explaining the wave-induced changes in the mean horizontal velocity profiles are known so far. One is based on a 1DV local force balance neglecting lateral variations, and in the other secondary circulations in the cross-section are essential. In order to find out which phenomenon is dominant a 2DV numerical flow model based on the GLM formulation has

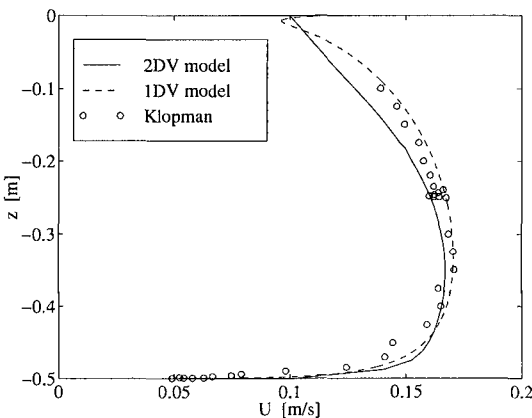


Figure 8: Mean streamwise horizontal velocity profile in center of a 5 m wide flume for waves following the current.

been developed. It is still in a preliminary state and the numerical results obtained so far are not always satisfactory.

Numerical experiments with the 2DV model for a 1 m and a 5 m wide flume give almost similar predictions of the mean horizontal velocity in streamwise direction in the center of the flume and a significant difference for the order of magnitude of the circulations. One might therefore conclude that phenomena in streamwise direction are dominant over those in lateral direction. However, the 2DV model overpredicts the velocity components in vertical and lateral direction measured by Klopman (1997). Two possible reasons are given here. Firstly, the computations have been carried out on a regular grid with a grid size of 1 cm, which was too coarse to represent the side-wall boundary layers well. These are only a few millimeters thick (order  $\beta^{-1}$ ). An irregular grid which is finer towards the boundaries has already been implemented. Results of these numerical experiments will be reported in the future.

Secondly, in the formulation of wave effects in the partial slip conditions and the  $k - \varepsilon$  turbulence model, the simplest approaches have been applied. GLM quantities are computed by Eulerian based models. Transformations from GLM to Eulerian and vice versa have been carried out only at the beginning and at the end of those processes. Improvement of this approach might lead to better results for the circulations.

Furthermore, extra attention has to be paid to the mean horizontal velocity profile for the situation of opposing waves. Towards the free surface a completely deviant behavior was observed compared to the measurements and

predictions with the 1DV model. The cause of this is unknown for now and will be considered carefully in the near future.

### Acknowledgements

This research is supported by the Technology Foundation (STW), The Netherlands. Furthermore, we would like to thank G. Klopman and M.W. Dingemans for their valuable suggestions, and Delft Hydraulics for putting their numerical solver at our disposal.

### References

- Andrews, D.G. & McIntyre, M.E. 1978. An exact theory of nonlinear waves on a Lagrangian-mean flow. *J. Fluid Mech.*, **89**, 609–646.
- Dingemans, M.W. 1997. *Water wave propagation over uneven bottoms*. World Scientific, Singapore.
- Dingemans, M.W., van Kester, J.A.Th.M., Radder, A.C. & Uittenbogaard, R.E. 1996. The effect of the CL-vortex force in 3D wave-current interaction. *Pages 4821–4832 of: Proc. 25th Int. Conf. on Coastal Engng, Orlando*. ASCE, New York.
- Grant, W.D. & Madsen, O.S. 1979. Combined wave-current interaction with a rough bottom. *J. Geophys. Res.*, **84**(C4), 1797–1808.
- Groeneweg, J. & Klopman, G. 1998. Changes of the mean velocity profiles in the combined wave-current motion described in a GLM formulation. *J. Fluid Mech.*, **370**, 271–296.
- Kemp, P.H. & Simons, R.R. 1982. The interaction of waves and a turbulent current; waves propagating with the current. *J. Fluid Mech.*, **116**, 227–250.
- Kemp, P.H. & Simons, R.R. 1983. The interaction of waves and a turbulent current; waves propagating against the current. *J. Fluid Mech.*, **130**, 73–89.
- Klopman, G. 1994. *Vertical structure of the flow due to waves and currents*. Tech. rept. H840.32, Part 2. Delft Hydraulics.
- Klopman, G. 1997. *Secondary circulation of the flow due to waves and current*. Tech. rept. Z2249. Delft Hydraulics.

- Leibovich, S. 1983. The form and dynamics of Langmuir circulations. *Ann. Rev. Fluid Mech.*, **15**, 391–427.
- McIntyre, M.E. 1980. Towards a Lagrangian-mean description of stratospheric circulation and chemical transports. *Phil. Trans. R. Soc. Lond.*, **A296**, 129–148.
- Mei, C.C., Liu, P.L.-F. & Carter, T.G. 1972. *Mass transport in water waves*. Tech. rept. 146. M.I.T. Rep. Ralph M. Parsons Lab. Water Resources Hydrodynamics.
- Nielsen, P. & You, Z-J. 1996. Eulerian mean velocities under non-breaking waves on horizontal bottoms. *Pages 4066–4078 of: Proc. 25th Int. Conf. on Coastal Engng, Orlando*.
- Van Kester, J.A.Th.M., Uittenbogaard, R.E. & Dingemans, M.W. 1996. *The effect of the CL-vortex force in 3D wave-current interaction*. Tech. rept. Z751. Delft Hydraulics.